Dual-Layer Characteristic Temperature Model for AWES Dynamic Thermal Detection Based on IR

Zixuan Shangguan[1,2] and Cunman Zhang[1,2(✉)]

[1] School of Automotive Studies, Tongji University, Shanghai 201804, China
zhangcunman@tongji.edu.cn
[2] Clean Energy Automotive Engineering Center, Tongji University, Shanghai 201804, China

Abstract. With the increasing application of the AWES, the dynamic thermal detection of the electrolyzer inspires great interest. The dimension of dynamic thermal detection of the AWES is currently limited to only the inlet and outlet temperatures. This study proposes a dual-layer characteristics temperature model for AWES temperature monitoring. The DLCT model deals with the difficulty of extracting characteristic temperature with its first layer of multi gaussian distribution regression. The second layer model can clarify the disturbing signal using linear regression and provide a quantized temperature distribution pattern of the surface temperature. This DLCT model does not require additional modifications to the AWES, nor any temperature sensor inside or on its surface. With the DLCT model implemented during dynamic operation, the AWES can be more comprehensive monitored, and more insights can be gathered regarding the DLCT for better thermal uniformity.

Keywords: Alkaline electrolyzer · Dynamic thermal detection · Characteristic temperature · Multi gaussian regression · Machine learning

1 Introduction

Hydrogen energy system can replace the fossil fuel system as a solution for many global environmental issues, and water-electrolysis-based hydrogen production has gain its maturity in term of both technology [1] and economic [2]. The alkaline water electrolysis system (AWES) is one of the most widely used, technically mature and cost-effective high-power water electrolysis hydrogen production technology [1]. The AWES is considered to be able to provide medium term large-scale Renewable Energy-based green hydrogen for the hydrogen energy system [3]. However, the fluctuating power output of the renewable power system requires AWES to operate under similar unsteady conditions, which brings up the necessity of thermal detection over AWES for more detailed dynamic response. As status quo, in the operation and maintenance of AWES, the only thermal parameters recorded are normally inlet and outlet temperature for the electrolyzer.

H. Sun et al. (Eds.): WHTC 2023, SPPHY 393, pp. 76–82, 2024.
https://doi.org/10.1007/978-981-99-8631-6_8

For the dynamic thermal detection of AWES, only recording the inlet and outlet temperature means only acquiring the temperature of the inlet fluid and the gas-liquid mixture at two positions on the end-face of the electrolyzer. The temperature of the bulk structure is not recorded, neither on the surface nor from the inside. Such a lack of understanding of dynamic thermal detection leads to the inability for the uniformity of its temperature distribution and may even cause the ignorance of its inside hot spots. In addition, the limit of indicative temperature also leads to over-simplification of the evaluation criteria of the electrolyzer and brings difficulties in collecting sufficient temperature distribution data over the dynamic operating conditions. In conclusion, only recording the inlet and outlet temperature of the electrolyzer makes it difficult to understand the thermal characteristics of the AWES, and, also, to provide more improvement guidance as well as more analysis dimensions for the AWES, such as multi-physics approaches [4, 5].

Hence, this study puts forward the dual-layer characteristic temperature (DLCT) model, which is composed of two layers of the characteristic temperature (CT) regression analysis over the side surface of the electrolyzer.

2 Modeling Method

As demonstrated in Fig. 1(a), the IR recorder is stationed to the side of the electrolyzer, the captured IR image is drawn in Fig. 1 (b). As can be seen, due to characteristics of the lye-gas mixture in the electrolyzer [5], the temperature is higher in the upper region of the electrolyzer. The temperature of the metal plate (70.4 °C) is quite higher than the gasket region (57.52 °C) in its adjacency. This unevenness is the first problem to be dealt with, in collecting the CT of the electrolyzer surface. And there are the current collectors with higher temperatures near the bottom, the CT analysis must be able to distinguish these disturbing signals.

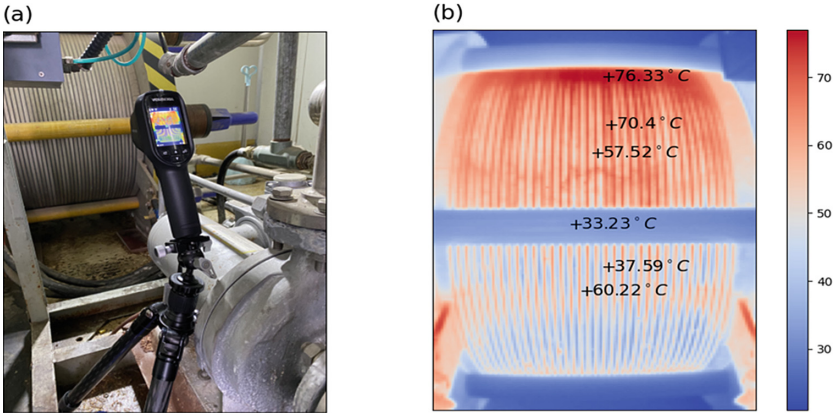

Fig. 1. (a) The apparatus of the infrared image collection, and (b) the recorded IR image with temperature noted at different locations.

The second problem comes with the obstacles and auxiliary parts on the electrolyzer. As in Fig. 1 (b), the clamping bolts of the electrolyzer are positioned at the top, middle and the bottom blocking the direction detection of the surface temperature. With larger rated power, the AWES grows in size, and the number of clamping bolts also grows, leading to more blocked surface area. And finally, the model should filter out the obstacles and provide the overall surface temperature distribution with quantized parameters.

This study aims to tackle these two problems with two layers of CT analysis model. The first layer CT model can extract the CT of the metal structure within the segment of the IR image, implemented with MGD regression. The second layer model can clarify the disturbing signal using linear regression, resume the surface temperature over the side of the electrolyzer and provide an overall quantized temperature distribution pattern of the surface temperature of the electrolyzer. This DLCT model does not require additional modifications to the AWES, nor does it attach any temperature sensor inside or on the surface of the electrolyzer.

3 First-Layer Characteristic Temperature Model

The IR image is first segmented as in Fig. 2 (a). The image is segmented into 12 vertical segments as demonstration, and the IR image can also be horizontally segmented or divided into a mesh grid.

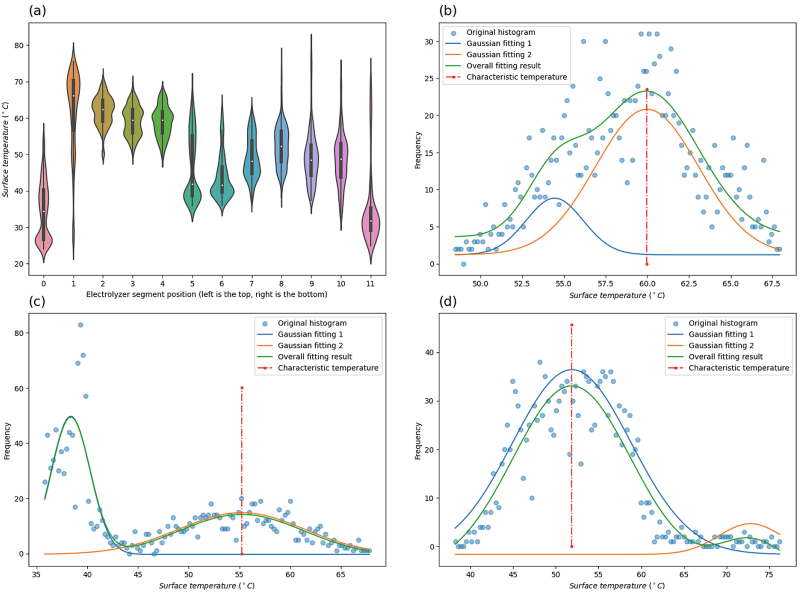

Fig. 2. (a) The violin graphs of each segment in an IR image, (b) the temperature distribution and MGD analysis results of segment No. 4, (c) the temperature distribution and MGD analysis results of segment No. 5, and (d) the temperature distribution and MGD analysis results of segment No. 8.

3.1 Multi-Gaussian Distribution Analysis

Here, MGD regression is performed to extract the CT within each segment. The gaussian distribution is also called the normal distribution [6]. In this study, for convenience, the gaussian distribution is converted to the frequency of occurrence, rather than probability. As a result, the temperature gaussian distribution formula can be changed into:

$$h(t) = h \times e^{-\frac{(t-t_0)^2}{2w^2}} + h_0 \tag{1}$$

In which, t represents temperature, $h(t)$ represents the frequency of occurrence of a certain temperature within in the adjacency of t. h represents the height of the frequency peak and is used to determine the significance of this distribution. t_0 is the expectation of the distribution, and the potential CT in the segment. w represents the width of the gaussian distribution and the h_0 represents the bottom noise of the segment.

However, as in Fig. 2 (b), (c), (d) the complexity of the distribution within on segment does not fit a single gaussian distribution. Hence, this study combines several gaussian distributions into the MGD model [7]. Within each segment, the distribution of the temperature signals can be described by:

$$h_i(t) = h_1 \times e^{-\frac{(t-t_{0,1})^2}{2w_1^2}} + h_2 \times e^{-\frac{(t-t_{0,2})^2}{2w_2^2}} + h_3 \times e^{-\frac{(t-t_{0,3})^2}{2w_3^2}} + h_0 \tag{2}$$

$(h_1, t_{0,1}, w_1)$, $(h_2, t_{0,2}, w_2)$ and $(h_3, t_{0,3}, w_3)$ three sets of parameters represent the relevant parameters of three Gaussian distributions, among which $t_{0,1}$, $t_{0,2}$, $t_{0,3}$ are the three potential CT of the region. In this paper, SciPy based on python is used to carry out the regression of the above equation [8].

3.2 First Layer CT Model Results

The result CTs within each segment come from the actual surface of the electrolyzer. For in Fig. 2 (b) and compared with Fig. 1 (b), the higher CT represents the temperature of the metal plate, whereas the lower CT represents the gasket. Likewise, the clamping bolts, and the current collectors, can also be screened out of the CTs. Finally, the CT with higher height of frequency of occurrence is chosen as the CT of the temperature of this segment. Likewise, in Fig. 2 (c), the lower, however, more concentrated represents the clamping bolts at the middle in Fig. 1 (b), and the peak with higher temperature is the surface of the electrolyzer, which is recognized as the CT of the segment. And in the Fig. 2 (d), there are also two peaks in the figure. The peak with higher CT represents the hot current collectors near the bottom of the IR image, and the lower peak represents the surface temperature of the electrolyzer and should be acknowledged as the CT of the segment.

4 Second-Layer Characteristic Temperature Model

4.1 Regression Method

The potential CTs of each segment of the IR image are plotted in the Fig. 3(a), and CTs have been selected. In the top and bottom segment, there is no CT of the surface because a large proportion of the image is taken up by the clamping bolts and background. Rest

of the segments have CT on the surface, except segment No. 6 where the clamping bolt is dominant. And the linear relationship between CTs on the electrolyzer surface and segment positions is explicit.

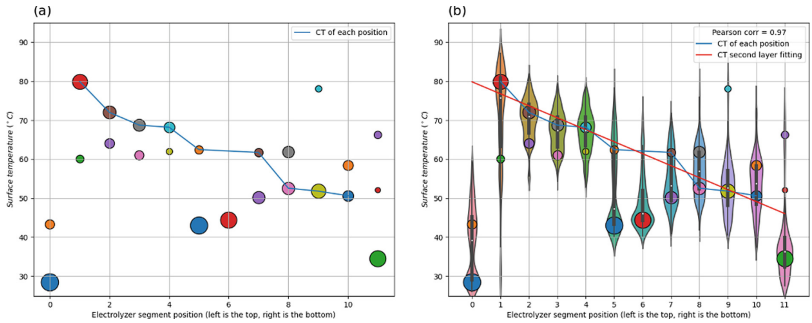

Fig. 3. **(a)** The potential CTs of each segment, and (b) the result of the second layer CT model.

Hence linear regression should be applied to analyze the distribution pattern. The temperature distribution of each segment on the electrolyzer surface can be expressed as:

$$T_i = a \times x_i + b, i \in [1, n] \tag{3}$$

In which, T_i represents the CT of a certain segment, $x_i \in N$ represents the position of the segment, and $a, b \in R$ are the parameters for the temperature distribution pattern. a Stands for the slope of the linear equation and b for the intercept. This study also employs the built-in method from SciPy to conduct the second layer CT model.

4.2 Second Layer CT Model Results

The Pearson correlation is 0.97, which means the segment position has a very strong linear relationship with the CT [9]. As shown in the Fig. 3(b), the slope of the linear relationship between CT and segment position is − 3.06, which means every time we check one segment just beneath another, the CT will likely be 3.06 °C lower. The intercept of the equation is 79.80 °C, which means based on the estimation of the second-layer model, the CT on the top of the electrolyzer surface will be near 80 °C. And the CT s of any other segments hindered by obstacles can be derived from this linear relationship.

More importantly, the second-layer CT model provides us with the quantized temperature distribution pattern on the electrolyzer surface, which can be introduced to examine the thermal uniformity of the electrolyzer design and operation. The slope in linear regression can describe the significance of the temperature variation of the electrolyzer, and the intercept can predict the maximum temperature on the electrolyzer surface.

5 Conclusion

In summary, this study introduces the DLCT model to deal with two major problems of AWES dynamic thermal detection, the extraction of characteristic temperatures and hinderance of auxiliaries. The first layer employs MGD regression to evaluate the segment temperature and produces multiple potential CTs. The CT is then selected for each segment, and fed into the second layer, where linear regression is implemented to provide quantized distribution pattern.

And the results of the DLCT not only provide global AWES CT, but also quantized temperature distribution pattern, which will bring in richer dimensions for detecting and optimizing the dynamic operation of the electrolyzer. As a result, the AWES can be more comprehensive monitored during dynamic operation, and more guidance can be gathered with the DLCT for better thermal uniformity.

References

1. Bodner, M., Hofer, A., Hacker, V.: H2 generation from alkaline electrolyzer. Wiley Interdisc. Rev. Energy Environ. **4**, 365–381 (2015)
2. Bowen Yang, R.Z., Zhang, C.: The techo-economic evaluation of hydrogen production cost towards anion exchange membrane electrolyzer. In: 23rd World Hydrogen Energy Conference Proceedings; Track **15**, 1376–1378 (2022)
3. Chang Zhang, J.W., Ren, Z., Yu, Z., Wang, P.: Wind-powered 250 kW electrolyzer for dynamic hydrogen production: a pilot study. Int. J. Hydrogen Energy **46**, 34550–34564 (2021)
4. Le Bideau, D., Mandin, P., Benbouzid, M., Kim, M., Sellier, M.: Review of necessary thermophysical properties and their sensivities with temperature and electrolyte mass fractions for alkaline water electrolysis multiphysics modelling. Int. J. Hydrogen Energy **44**, 4553–4569 (2019)
5. Hammoudi, M., Henao, C., Agbossou, K., Dubé, Y., Doumbia, M.L.: New multi-physics approach for modelling and design of alkaline electrolyzers. Int. J. Hydrogen Energy **37**, 13895–13913 (2012)
6. Do, C.B.: The multivariate Gaussian distribution. Section Notes, Lecture on Machine Learning, CS, 229 (2008)
7. Ahrendt, P.: The Multivariate Gaussian Probability Distribution. Technical University of Denmark, Tech Report, 203 (2005)
8. Virtanen, P., Gommers, R., Oliphant, T.E., Haberland, M., Reddy, T., Cournapeau, D., et al.: SciPy 1.0: fundamental algorithms for scientific computing in python. Nat. Methods **17**, 261–272 (2020)
9. Benesty, J., Chen, J., Huang, Y., Cohen, I.: Pearson Correlation Coefficient. Noise Reduction in Speech Processing, pp. 1–4. Springer (2009)